

 Open access • Journal Article • DOI:10.1039/C4CP00482E

## **Easily-prepared dinickel phosphide (Ni<sub>2</sub>P) nanoparticles as an efficient and robust electrocatalyst for hydrogen evolution. — [Source link](#)**

[Ligang Feng](#), [Heron Vrubel](#), [Michaël Bensimon](#), [Xile Hu](#)

**Institutions:** [École Polytechnique Fédérale de Lausanne](#)

**Published on:** 05 Mar 2014 - [Physical Chemistry Chemical Physics](#) (The Royal Society of Chemistry)

**Topics:** [Electrocatalyst](#), [Phosphide](#) and [Catalysis](#)

Related papers:

- [Nanostructured Nickel Phosphide as an Electrocatalyst for the Hydrogen Evolution Reaction](#)
- [Self-Supported Nanoporous Cobalt Phosphide Nanowire Arrays: An Efficient 3D Hydrogen-Evolving Cathode over the Wide Range of pH 0–14](#)
- [Solar Water Splitting Cells](#)
- [Highly active electrocatalysis of the hydrogen evolution reaction by cobalt phosphide nanoparticles.](#)
- [MoS<sub>2</sub> Nanoparticles Grown on Graphene: An Advanced Catalyst for the Hydrogen Evolution Reaction](#)

Share this paper:    

View more about this paper here: <https://typeset.io/papers/easily-prepared-dinickel-phosphide-ni2p-nanoparticles-as-an-4vjoowe4vz>

## Electronic Supplementary Information

### **Easily-prepared dinickel phosphide (Ni<sub>2</sub>P) nanoparticles as an efficient and robust electrocatalyst for hydrogen evolution**

Ligang Feng,<sup>a</sup> Heron Vrabel,<sup>a</sup> Michaël Bensimon<sup>b</sup> and Xile Hu<sup>a,\*</sup>

<sup>a</sup>Laboratory of Inorganic Synthesis and Catalysis, Institute of Chemical Sciences and Engineering, <sup>b</sup>General Environmental Laboratory, Institute of Environmental Engineering Ecole Polytechnique Fédérale de Lausanne (EPFL), SB-ISIC-LSCI, BCH 3305, Lausanne, CH 1015, Switzerland

\* To whom correspondence should be addressed. E-mail: [xile.hu@epfl.ch](mailto:xile.hu@epfl.ch)

## Chemicals and Reagents

$\text{NiCl}_2 \cdot 6\text{H}_2\text{O}$  (Reagent plus) were purchased from Aldrich and stored under nitrogen.  $\text{NaH}_2\text{PO}_2$  (analysis grade) were purchased from Acros and stored under nitrogen. Unless noted, all other reagents were purchased from commercial sources and used without further purification. It should be noted that all solutions in our work were prepared using Millipore-MiliQ water (resistivity :  $\rho \geq 18 \text{ M}\Omega \text{ cm}^{-1}$ ) and the reagents used were analytical-grade.

## Preparation of $\text{Ni}_2\text{P}$ nanoparticles

A solid mixture of 0.66 g  $\text{NaH}_2\text{PO}_2$  and 0.3 g  $\text{NiCl}_2 \cdot 6\text{H}_2\text{O}$  was mechanically grounded using a mortar and pestle in the glove box (to prevent deliquescence; not absolutely necessary). After that, the solid mixture was transferred to a quartz tube, where it was heated to 250 °C in a tubular oven and kept for 1 h in a flowing 30 mL/min  $\text{N}_2$ . Following cooling to room temperature in a continuous  $\text{N}_2$  flow, the  $\text{Ni}_2\text{P}$  particles were passivated in a 1.0 mol%  $\text{O}_2/\text{N}_2$  mixture at 20 mL/min for 1 h. Finally, the products were washed with water and dried at room temperature. The synthesis is similar to that reported in Catalysis Communications, 2011, 12, 1157, except that  $\text{NaH}_2\text{PO}_2$  rather than  $\text{NaH}_2\text{PO}_3$  is used. The latter is not available to us.

## Physical methods

Energy Dispersive X-Ray Spectroscopy (EDX) was taken in a Phillips (FEI) XLF-30 FEG scanning electron microscope. XRD measurements were carried out on a X'Pert Philips diffractometer in Bragg-Brentano geometry with  $\text{Cu K}_{\alpha 1}$  radiation and a fast Si-PIN multi-strip detector (0.1540 nm). TEM images were taken on a Philips (FEI) CM12 transmission electron microscope with a LaB6 source operated at 120 kV accelerating voltage. The Scherrer equation was used for crystal size calculation:  $d = K\lambda/\beta\cos(\theta)$ .  $K$  is the shape factor with a typical value of about 0.9,  $\lambda$  is the X-ray wavelength, i.e., 1.54056 Å here,  $\beta$  is the full width at half maximum (FWHM) in radians, and  $\theta$  is the Bragg angle,  $d$  is the mean size of the ordered (crystalline) domains, which may be smaller or equal to the grain size.

The Inductively Coupled Plasma Mass spectrometry (ICP-MS) ICP-MS instrument used in this work was the Finnigan<sup>TM</sup> Element2 High Performance High Resolution ICP-MS, which consists of a double focusing reverse geometry mass spectrometer. The sensitivity was better than

$1.2 \times 10^5$  cps/ppb of  $^{115}\text{In}$  at a mass resolution of 4000, which corresponds to  $1.2 \times 10^6$  cps/ppb at low resolution mode of 500. Measurement repeatability expressed in terms of RSD was better than 5%, depending on the element. The accuracy of the method was tested using certified riverine water reference materials SLRS-3. Accuracy was better than 5%. The detection limits obtained for trace metals in the Medium resolution mode ( $R=4000$ ) without the influence of signal interferences were in routine mode less than  $0.2 \text{ ng l}^{-1}$  for all elements. Calibration standards were prepared through successive dilutions in cleaned Teflon bottles, of  $1 \text{ g l}^{-1}$  ICPMS stock solutions ( Bernd Kraft ). Suprapur® grade nitric acid (65% Merck) was used for the dilution of samples and for the preparation of standards (2+1000). Ultrapure water was produced using Milli-Q® Ultrapure Water System (Millipore, Bedford, USA). The mass resolution was set to 4000 in order to use the ability of the high resolution technique to resolve most spectral interferences from the analyte ions observed for Ni. The high resolution mode is also useful for samples having unexpected or unknown interferences, because the quantification is obtained by integrating only the area of the analyte peak, without the influence of an unexpected interference peak.

### **Fabrication of working electrodes**

$\text{Ni}_2\text{P}$  particles were dispersed by sonication of a 1 mL ethanol solution containing 50  $\mu\text{L}$  Nafion solution (5 wt%, Aldrich Co. USA). 10  $\mu\text{L}$  of the above solution was pipetted and spread on a mirror-finished glassy carbon electrode. The glassy carbon electrode was polished with alumina slurry (0.5 and 0.03  $\mu\text{m}$ ) successively before use. The modified electrode was dried at room temperature for 30 min. The apparent surface area of the glassy carbon electrode was  $0.07 \text{ cm}^2$ . The Nickel electrode with a surface area of  $0.03 \text{ cm}^2$  was used for comparison. Nickel hydroxide electrode was prepared by electrodeposition method in a 0.1 M  $\text{Ni}(\text{NO}_3)_2$  solution using glassy carbon electrode as the working electrode. The reduction current was  $1 \text{ mA cm}^{-2}$  and the deposition was carried out for 60 s. The measurements were carried out at room temperature in 1 M  $\text{H}_2\text{SO}_4$  or 1 M KOH solution with a scan rate of  $5 \text{ mV s}^{-1}$ .

For the study of the dissolution of  $\text{Ni}_2\text{P}$ , a large pellet disk electrode was used. 0.25 g of powdered  $\text{Ni}_2\text{P}$  was mixed with 0.150 g of Teflon powder (1 $\mu\text{m}$ ). The mixture was pressed in a conventional KBr pelletizer under 10 Tons to produce a 12 mm diameter pellet. A copper wire

contact was glued to one side of the pellet using silver conductive epoxy glue (CircuitWorks CW2400 - Chemtronics). A 5 mm hole mask was glued to the other side of the electrode to limit the surface area. With the exception of the active area, the whole body of the electrode was insulated with molten polypropylene.

### **Electrochemical measurements**

Electrochemical measurements were recorded by a Gamry Instruments Reference 600 potentiostat. A traditional three-electrode configuration was used. For polarization and electrolysis measurements, a platinum wire was used as the auxiliary electrode and an Ag/AgCl (KCl saturated) electrode was used as the reference electrode. Potentials were referenced to a reversible hydrogen electrode (RHE) by adding a value of  $(0.197 + 0.059\text{pH})$  V. Ohmic drop correction was performed using the current interrupt method. A total liquid volume of 50 mL was used to fill the cell. The platinum counter electrode was separated from the solution through a porous glass frit (porosity 3) and this whole assembly inserted into one side of the H cell. The modified working electrode was inserted in the other side of the cell, together with a magnetic stirring bar and a Luggin capillary.

For the ICP-MS measurement of dissolution of Ni<sub>2</sub>P, 1 mL of the electrolyte solution under electrolysis was sampled at different hours and stored in the refrigerator before test.

### **Hydrogen production yield**

The yield of hydrogen is determined using our previously established procedure (e.g. Chem. Sci. 2011, 2, 1262). Two small inlets were present in the cell allowing the connection to the pressure monitoring device and the other kept closed by a septum for sampling of the gas phase. The whole cell apparatus is gas-tight and the pressure increase is proportional to the gases generated (H<sub>2</sub> + O<sub>2</sub>). Prior to each experiment, the assembled cell was calibrated by injecting known amounts of air into the closed system and recording the pressure change. Pressure measurements during electrolysis were performed using a SensorTechnics DSDX0500D4R differential pressure transducer. Pressure data was recorded using an A/D Labjack U12 interface with a sampling interval of 1 point per second. The electrolysis was conducted at fixed potential and the solution was stirred with a magnetic stir bar during test.

After the calibration the cell was purged with nitrogen for 20 minutes and the measurements were performed. The Faradaic yield was calculated as follow:

The total amount of charge (Q) passed through the cell was obtained from the current-potential curve. The total amount of hydrogen produced (x) was measured using the pressure sensor. Assuming 2 electrons are needed to make one H<sub>2</sub> from two protons. Faradaic yield for H<sub>2</sub> =  $Q/2xF$ .

**Table S1.** Comparison of non-precious HER catalysts. Note that the specific surface of the different catalysts was not controlled for and thus, the estimates are quite crude and may not be reflective of the differences in specific activity.

catalysts	Condition	Loading	Overpotential @ 20 mA cm <sup>-2</sup>	Tafel slope (mV/dec)	Reference
Ni <sub>2</sub> P nanoparticles	1 M H <sub>2</sub> SO <sub>4</sub>	0.38 mg/cm <sup>2</sup>	0.14 V	87	This work
MoS <sub>2</sub> /RGO	0.5 M H <sub>2</sub> SO <sub>4</sub>	0.28 mg/cm <sup>2</sup>	0.17 V	41	[1]
Ni <sub>2</sub> P hollow particles	0.5 M H <sub>2</sub> SO <sub>4</sub>	1 mg/cm <sup>2</sup>	0.13V	81 ( $\eta > 125$ )	[2]
MoS <sub>2</sub> /SWCNTs	0.5 M H <sub>2</sub> SO <sub>4</sub>	0.136 mg/cm <sup>2</sup>	0.2 V	44.4	[3]
MoS <sub>2</sub>	0.5 M H <sub>2</sub> SO <sub>4</sub>	0.136 mg/cm <sup>2</sup>	0.23 V	56.4	[3]
MoS <sub>2+x</sub>	1 M H <sub>2</sub> SO <sub>4</sub>	0.2 mg/cm <sup>2</sup>	0.17V	40	[4]
MoS <sub>2</sub>	0.5 M H <sub>2</sub> SO <sub>4</sub>	0.06 mg/cm <sup>2</sup>	0.23V@10mA cm <sup>-2</sup>	50	[5]
NiMoN	0.1 M HClO <sub>4</sub>	0.25 mg/cm <sup>2</sup>	0.23V@5mA cm <sup>-2</sup>	35	[6]
MoB	1 M H <sub>2</sub> SO <sub>4</sub>	2.5 mg/cm <sup>2</sup>	0.23 V	55	[7]
Mo <sub>2</sub> C/CNT	0.1 M HClO <sub>4</sub>	2 mg/cm <sup>2</sup>	0.15V@10mA cm <sup>-2</sup>	55.2	[8]
Mo <sub>2</sub> C	1 M H <sub>2</sub> SO <sub>4</sub>	1.4 mg/cm <sup>2</sup>	0.23 V	56	[7]
WS <sub>2</sub> nanosheet	0.5 M H <sub>2</sub> SO <sub>4</sub>	0.1–0.2 $\mu$ g/cm <sup>2</sup>	0.3 V	60	[9]
WS <sub>2</sub> nanosheet	0.5 M H <sub>2</sub> SO <sub>4</sub>	0.285 mg/cm <sup>2</sup>	0.17 V	72	[10]
MoB	1 M KOH	2.3 mg/cm <sup>2</sup>	0.24 V	59	[7]
Mo <sub>2</sub> C	1 M KOH	0.8 mg/cm <sup>2</sup>	0.21 V	54	[7]
NiZn	1 M NaOH	--	0.25 V	119	[11]
NiZr	6 M KOH	--	0.30 V	110	[12]
Porous Ni <sub>3</sub> Al	6 M KOH	--	0.25 V	--	[13]
NiT <sub>i</sub>	1 M NaOH	--	0.17 V	283	[14]
Ni <sub>2</sub> P nanoparticles	1 M KOH	0.38 mg/cm <sup>2</sup>	0.25 V	100	This work

-- not reported in the literature

## References

- [1] Y. Li, H. Wang, L. Xie, Y. Liang, G. Hong, H. Dai, *J. Am. Chem. Soc.* **2011**, *133*, 7296-7299.
- [2] E. J. Popczun, J. R. McKone, C. G. Read, A. J. Biacchi, A. M. Wiltrout, N. S. Lewis, R. E. Schaak, *J. Am. Chem. Soc.* **2013**.
- [3] Y. Yan, X. Ge, Z. Liu, J.-Y. Wang, J.-M. Lee, X. Wang, *Nanoscale* **2013**, *5*, 7768-7771.
- [4] H. Vrubel, X. Hu, *ACS Catalysis* **2013**, *3*, 2002-2011.
- [5] J. Kibsgaard, Z. B. Chen, B. N. Reinecke, T. F. Jaramillo, *Nat. Mater.* **2012**, *11*, 963-969.
- [6] W. F. Chen, K. Sasaki, C. Ma, A. I. Frenkel, N. Marinkovic, J. T. Muckerman, Y. M. Zhu, R. R. Adzic, *Angew. Chem. Int. Ed.* **2012**, *51*, 6131-6135.
- [7] H. Vrubel, X. L. Hu, *Angew. Chem. Int. Ed.* **2012**, *51*, 12703-12706.

- [8] W. F. Chen, C. H. Wang, K. Sasaki, N. Marinkovic, W. Xu, J. T. Muckerman, Y. Zhu, R. R. Adzic, *Energy Environ. Sci.* **2013**, *6*, 943-951.
- [9] D. Voiry, H. Yamaguchi, J. W. Li, R. Silva, D. C. B. Alves, T. Fujita, M. W. Chen, T. Asefa, V. B. Shenoy, G. Eda, M. Chhowalla, *Nat. Mater.* **2013**, *12*, 850-855.
- [10] Z. Wu, B. Fang, A. Bonakdarpour, A. Sun, D. P. Wilkinson, D. Wang, *Appl. Catal. B: Environ.* **2012**, *125*, 59-66.
- [11] Z. Zheng, N. Li, C. Q. Wang, D. Y. Li, F. Y. Meng, Y. M. Zhu, *J. Power Sources* **2013**, *222*, 88-91.
- [12] L. Mihailov, T. Spassov, M. Bojinov, *Int. J. Hydrogen Energy* **2012**, *37*, 10499-10506.
- [13] L. Wu, Y. He, T. Lei, B. Nan, N. Xu, J. Zou, B. Huang, C. T. Liu, *Mater. Chem. Phys.* **2013**, *141*, 553-561.
- [14] A. Kellenberger, N. Vaszilcsin, W. Brandl, N. Duteanu, *Int. J. Hydrogen Energy* **2007**, *32*, 3258-3265.



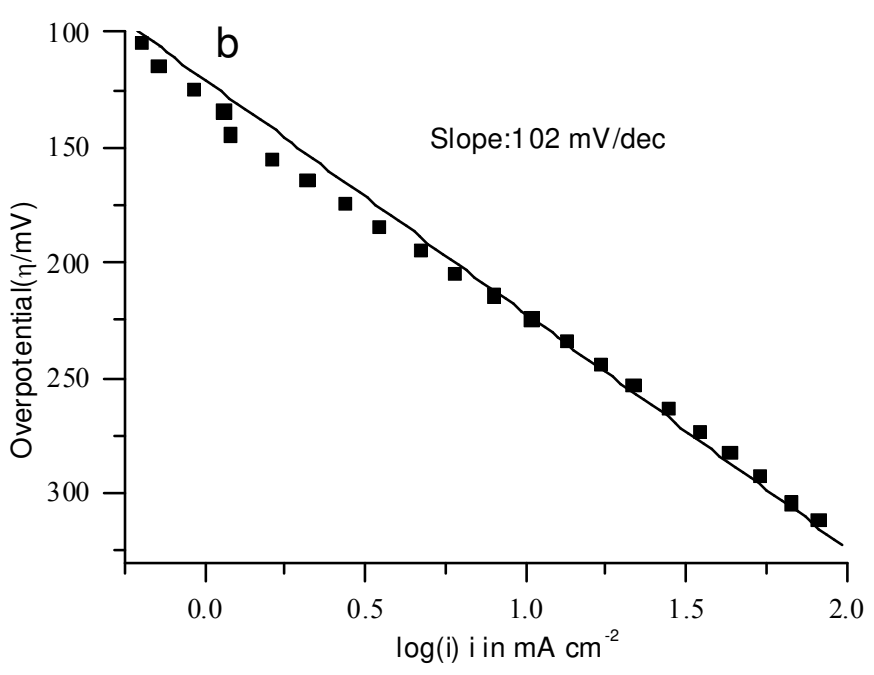
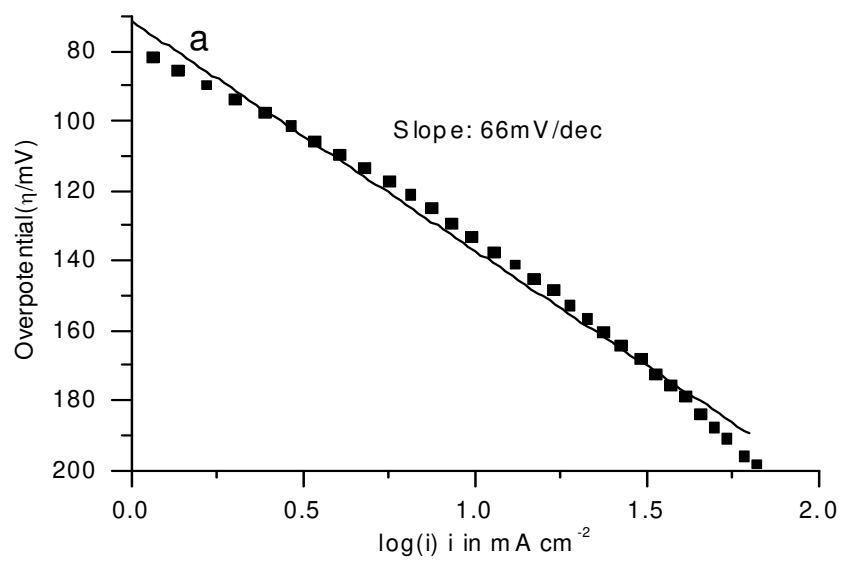


**Figure S1.** Tafel slopes of HER catalyzed by Ni<sub>2</sub>P obtained from polarization curves in (a) 1 M H<sub>2</sub>SO<sub>4</sub>; (b) 1 M KOH.

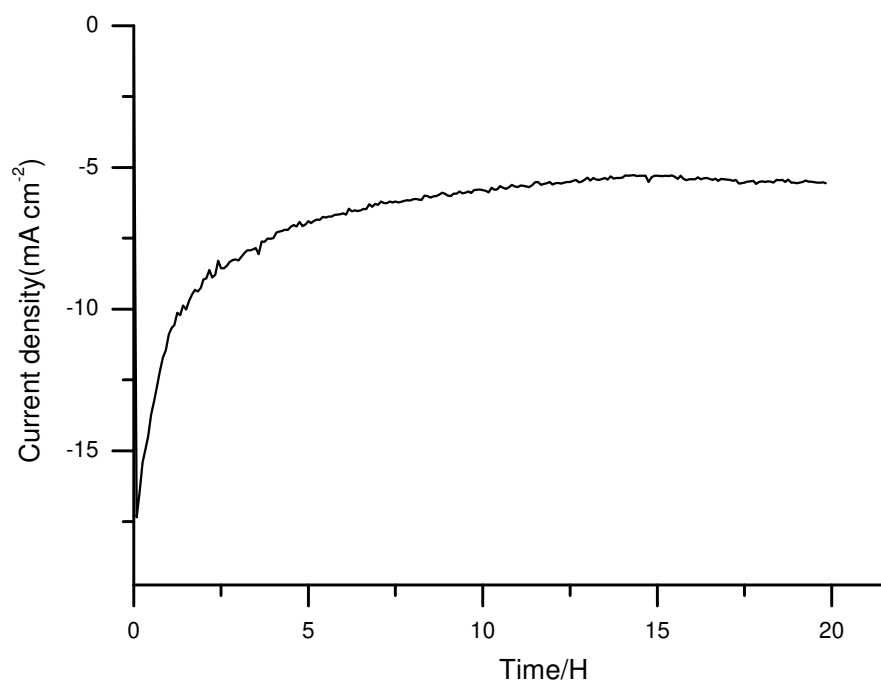


**Figure S2.** Time dependence of the catalytic current for a Ni<sub>2</sub>P/Ti foil electrode during potentiostatic electrolysis over 20 hours at -0.15 V in 1 M H<sub>2</sub>SO<sub>4</sub>. Loading: 0.25 mg/cm<sup>2</sup>.

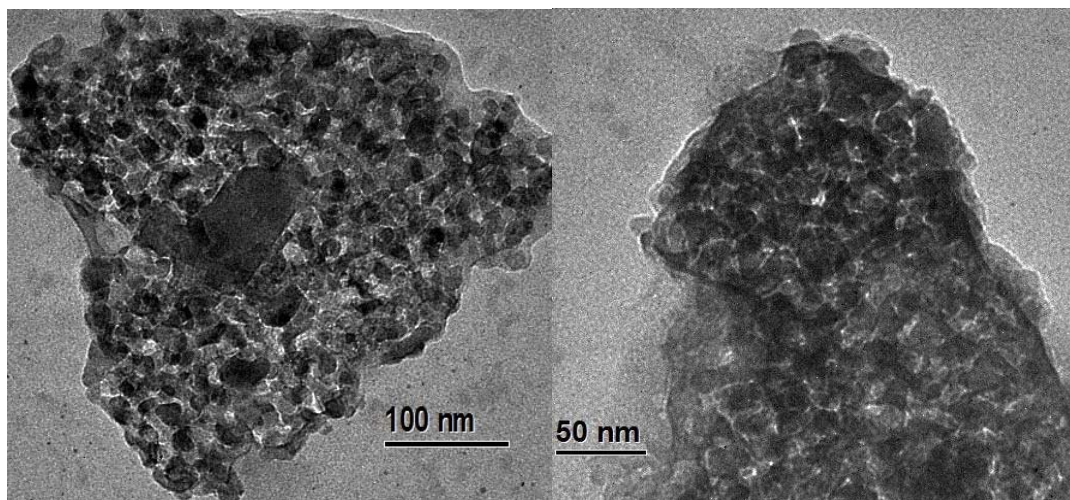


**Figure S3a.** TEM images of  $\text{Ni}_2\text{P}$  particles after electrolysis for 48 hours electrolysis at  $13 \text{ mA cm}^{-2}$ . The particles were removed from the electrode before analysis.

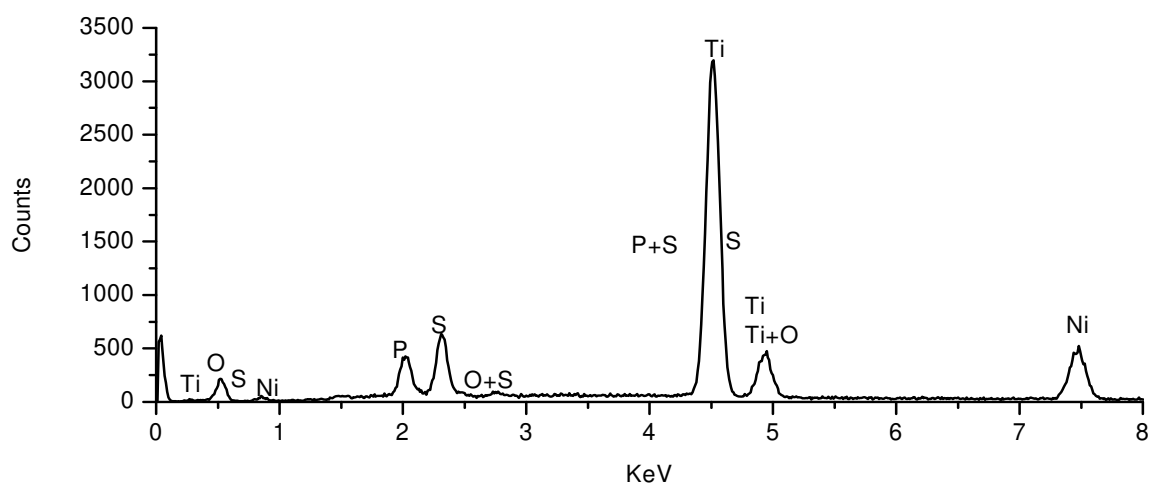


**Figure S3b.** EDX spectrum of  $\text{Ni}_2\text{P}$  particles after electrolysis for 48 hours electrolysis at  $13 \text{ mA cm}^{-2}$ . The particles were removed from the electrode before analysis. Atomic ratio:  $\text{Ni/P}=1.94$ . S is from the  $\text{H}_2\text{SO}_4$  and Ti is from the support where EDX is done.

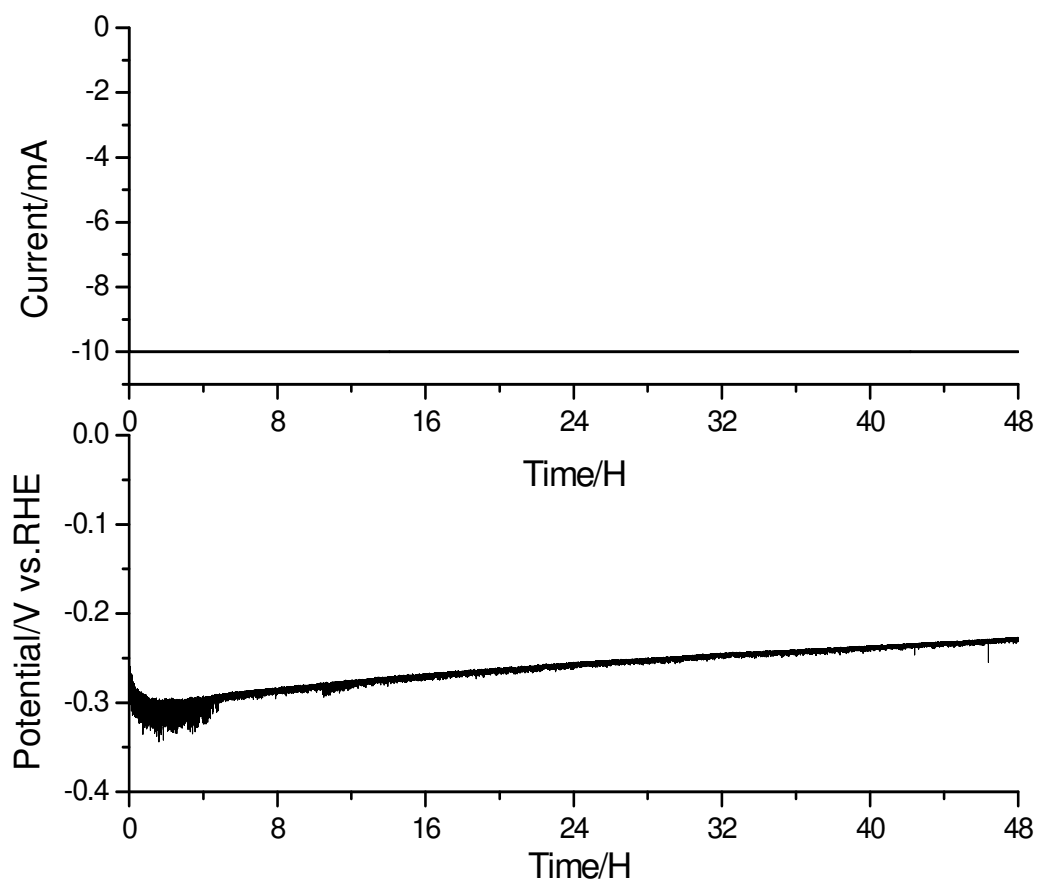


**Figure S4.** Accelerated stability test for Ni<sub>2</sub>P particles on a glassy carbon electrode. Loading: 0.38 mg/cm<sup>2</sup>. Top: Galvanostatic electrolysis at 140 mA/cm<sup>2</sup> for 48 hours. Bottom: the dependence of potential during this process. The small decrease of potential over time might be due to some electrochemical conditioning.

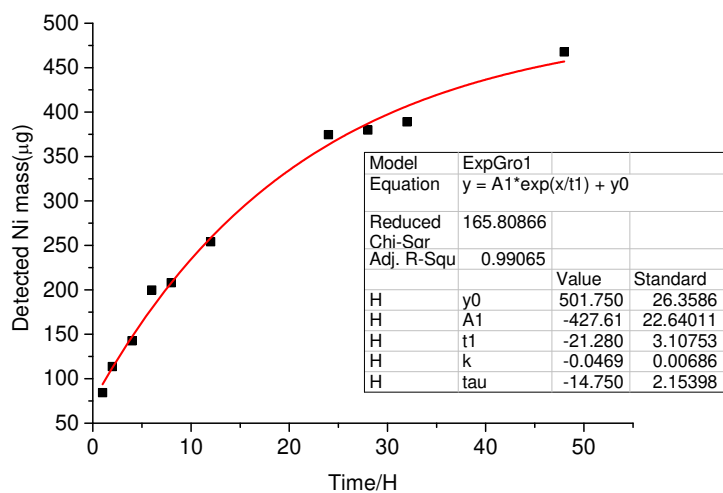


**Figure S5.** The amount of Ni detected in the electrolyte solution during electrolysis at  $10 \text{ mA/cm}^2$ . The electrode is a  $\text{Ni}_2\text{P}$  pellet with 250 mg  $\text{Ni}_2\text{P}$  (ca. 200 mg Ni). The data is fitted with an exponential growth function.